(or current). The stripe pattern disappears again (Fig. 4D) when the electric field is removed and the crystal returns back to the high-resistive state. By the atomic force microscope measurement, the surface of the stripe pattern region was confirmed to be flat within 50 nm in height and hence the stripes are not due to groove-like strains. The dark stripe perhaps comes from metallic patches, because the metallic or nondimerized TCNQ stack gives rise to a lower reflectivity in the visible region (*11*). With use of the sensitivity of the totally symmetric (a_g) mode molecular vibration [CN stretching (ν_{CN}) of TCNQ] to the dimeric (Peierls-like) distortion (*10*), the microscopic infrared spectroscopy (*12*) has confirmed that the dimerization is much reduced in the current-flowing region accompanying the stripe pattern, but less so in the nonstripe region (corresponding to the crystal edge part in Fig. 4B). Such a current-path region characterized as the alternative dark and bright regions can be viewed as the periodic phase-segregation into carrier-rich (dark) and -poor (bright) regions.

This stripe pattern formation may originate from the long-range Coulomb repulsion interaction between the generated carrier-rich regions. A current-flowing state is a nonequilibrium state out of the scope of thermodynamics, yet the current-induced coexistence of the carrier-rich (high-conducting) and carrier-poor (low-conducting) regions may be viewed as a sort of phase segregation. This is perhaps inherent to the correlated electron system like K-TCNQ, where the hypothetical metallic state is, in the sense of free energy, adjacent to the Mott-insulating state in spite of a seemingly large charge-gap. A specifically large dielectric constant along the stacking axis can effectively screen the Coulomb interaction between the carrier-rich regions, producing such a stripe pattern running perpendicular to the stacking axis, as we observed. Thus, we consider the observed phenomenon as one example of the self-organization in nonequilibrium systems as widely seen in natural systems and extensively investigated for several decades (*13*, *14*). A distinct feature is, however, that the stripe pattern in the present case is composed of electronically different phases, namely metallic (nondimerized) and poorly conducting (dimerized) states.

References and Notes

1. Z. G. Soos, *Annu. Rev. Phys. Chem.* **25**, 121 (1974).
2. L. R. Melby *et al.*, *J. Am. Chem. Soc.* **84**, 3374 (1962).
3. J. Siemons, P. E. Bierstedt, R. G. Kepler, *J. Chem. Phys.* **39**, 3523 (1963).
4. J. G. Vegter, T. Hibma, T. Kommandeur, *Chem. Phys. Lett.* **3**, 427 (1969).
5. N. Sakai, I. Shirotani, S. Minomura, *Bull. Chem. Soc. Jpn.* **45**, 3321 (1972).
6. H. Terauchi, *Phys. Rev. B* **17**, 2446 (1978).
7. Y. Lepine, A. Caillé, V. Larochelle, *ibid.* **18**, 3585 (1978).
8. Y. Iwasa *et al.*, *ibid.* **39**, 10441 (1989).
9. N. Watanabe, Y. Iwasa, T. Koda, *ibid.* **44**, 11111 (1991).
10. H. Okamoto, Y. Tokura, T. Koda, *ibid.* **36**, 3858 (1987).
11. K. Yakushi *et al.*, *Chem. Phys. Lett.* **68**, 139 (1979).
12. Y. Okimoto, R. Kumai, Y. Tokura, unpublished data.
13. G. Nicolis and I. Prigogine, *Self-Organization in Nonequilibrium Systems* (Wiley, New York, 1977).
14. T. Fukui and N. Kawakami, *Phys. Rev. B* **58**, 16051 (1998).

15. We thank N. Nagaosa, N. Kawakami, and H. Fukuyama for enlightening discussions. We also thank M. Izumi for his help with atomic force microscope measurements. This work, partly supported by New Energy and Industrial Technology Development Organization, was performed at JRCAT under the joint research agreement between National Institute for Advanced Interdisciplinary Research and Angstrom Technology Partnership.

24 November 1998; accepted 19 April 1999

Enhanced Reactivity of Highly Vibrationally Excited Molecules on Metal Surfaces

H. Hou,[1] Y. Huang,[2] S. J. Gulding,[2] C. T. Rettner,[1] D. J. Auerbach,[1]* A. M. Wodtke[2]*

The chemical dynamics of highly vibrationally excited molecules have been studied by measuring the quantum state–resolved scattering probabilities of nitric oxide (NO) molecules on clean and oxygen-covered copper (111) surfaces, where the incident NO was prepared in single quantum states with vibrational energies of as much as 300 kilojoules per mole. The dependence of vibrationally elastic and inelastic scattering on oxygen coverage strongly suggests that highly excited NO (v = 13 and 15) reacts on clean copper (111) with a probability of 0.87 ± 0.05, more than three orders of magnitude greater than the reaction probability of ground-state NO. Vibrational promotion of surface chemistry on metals (up to near-unit reaction probability) is possible despite the expected efficient relaxation of vibrational energy at metal surfaces.

Excited states of molecules are often much more reactive than ground-state species, in part because internal energy can help overcome barriers to reaction. Reactions of electronically excited molecules have been studied extensively; indeed, most of the field of photochemistry involves such states. The preparation and study of vibrationally excited reactants has proven more difficult. In polyatomic molecules, vibrational excitation may not remain localized in particular vibrations, and even in diatomic species, such states can prove difficult to prepare in large fluxes (*1*). These difficulties are particularly great for highly vibrationally excited molecules, where the vibrational excitation is a substantial fraction of the bond energy. The motivation to study the chemistry of such species is strong. The atoms in such molecules have large kinetic energies, which may enhance reaction rates. Furthermore, large amplitude vibration can distort the molecular electronic wave function, altering physical and chemical properties.

A few measurements of the reactivity of highly vibrationally excited molecules in the gas phase have been performed (*2*) and have shown that such excitation can produce reaction cross sections approaching the gas kinetic limit. Studies of the interactions of vibrationally excited molecules with surfaces have been restricted to low-lying vibrational states, populated either thermally (*3*) or with optical excitation (*4*). The reaction probabilities observed, although strongly influenced by vibration, were low (10^{-2}).

Unlike gas-phase reactions, it has not been clear that increasing the reactant vibrational excitation for reactions at surfaces can ever yield high reactivity. Particularly for metal surfaces, vibrational relaxation is potentially an important competitive channel. Indeed, theory predicts that vibrational relaxation rates will increase with the vibrational energy of the initial state (*5*, *6*) and thus could effectively thwart attempts to reach large reaction probabilities by using highly vibrationally excited molecules.

We present an experimental method that can reveal the chemical dynamics of highly vibrationally excited molecules at solid surfaces. We illustrate our approach using the model system of NO molecules interacting with a Cu(111) surface, where we observe a thousandfold vibrational enhancement of surface reactivity. In contrast, neither reagent translational energy nor surface temperature has a strong effect on the reaction probability

---

[1] IBM Research Division, Almaden Research Center, San Jose, CA 95120, USA. [2] Department of Chemistry, University of California, Santa Barbara, CA 93106, USA.

*To whom correspondence should be addressed.

over the range we have probed. The results are consistent with a "late" transition state (*7*) and illustrate the potential of this experimental approach for detailed studies of the transition-state dynamics of surface chemical reactions. We studied the scattering of NO molecules with vibrational states from $v = 13$ to $v = 22$ (vibrational energies of 290 and 390 kJ/mol). The narrow bandwidths of the lasers made it possible to populate a single rotation-vibration state with defined spin-orbit (Ω) and parity quantum numbers, so that the internal energy of NO before scattering was accurately known. Because the experimenter is freed from the limitations of the Boltzmann factor on the degree of vibrational energy available, a much broader range of surface chemical dynamics becomes accessible to experimental investigation. These results show that it is possible to promote surface reactivity to near-unit probability with vibrational excitation.

We prepared highly vibrationally excited NO with the use of stimulated emission pumping (SEP) (*1, 7*), as shown schematically in Fig. 1A. One laser, tuned to ω_{pump}, excites ground-state molecules to an intermediate electronically excited "stepping-stone" state, while a second laser, tuned to ω_{dump}, induces emission back down into a specific vibrationally excited level of the ground electronic state (*8*). The large structure change upon electronic excitation in many molecules allows good Franck-Condon overlap to high vibrational states in the two-photon transition. For example, the 24th excited vibrational state of NO, with vibrational energy of >400 kJ/mol, can be easily prepared by this method with efficiencies exceeding 1% (*7, 9*).

The apparatus used for the studies of vibrationally excited molecules at solid surfaces is shown in Fig. 1B. A pulsed molecular beam is skimmed and excited by the pump (*10*) and dump (*11*) lasers. A photomultiplier views the region where the laser beams cross the molecular beam, allowing fluorescence dip measurements (*12*) to characterize the optical excitation efficiency. The resulting highly vibrationally excited NO molecules then travel through a set of differential pumping apertures and enter the ultrahigh vacuum scattering chamber, where they collide with a Cu(111) surface at normal incidence.

Although the Cu(111) surface could easily be prepared free of oxygen by several cycles of Ar^+ sputtering and annealing, after the surface had been exposed to a molecular beam of ground-state NO for only a few minutes, a clear oxygen Auger electron spectroscopy (AES) signal (at 519 eV) was observed from the surface (*13*). Surface oxidation of copper by ground-state NO is well known and has been previously studied (*14*). At the surface temperatures used here (300 to 500 K), nitrogen is removed from the surface by subsequent surface reactions, and none was detected by AES (*15*). Stable and reproducible oxide surface overlayers of copper were readily prepared by exposure of the clean Cu(111) surface to NO_2, followed by elevation of the surface temperature to 800 K for several seconds. This procedure ensures that only chemisorbed oxygen atoms remain on the surface (*16*).

With the use of such a stable O-atom adlayer, we carried out a series of experiments designed to examine the inelastic energy transfer of highly excited NO with an oxidized copper surface. In these experiments, specific vibration-rotation states of NO were prepared using SEP (*9, 17*). Molecules that scattered from the surface were detected by 1+1 resonance enhanced multiphoton ionization (REMPI) (*18*). In this way, we have measured the vibrational-rotational state distributions as well as angular and kinetic energy distributions of inelastically scattered NO (*19*). Figure 2 shows a portion of the REMPI spectrum obtained when NO is initially prepared in $|v = 13, J = 2.5, \Omega = 0.5\rangle$ and the probe laser is tuned to detect molecules in the $v = 13$ state [probed through the $A(4) \leftarrow X(13)$ γ-band]. The solid line is the result of a least squares fit to the data points (*20*) using an experimentally determined laser line shape and theoretical (nonadjustable) transition frequencies and line strengths (*21*). A Boltzmann distribution of the $v = 13$ rotational states was used to simulate the rotational state populations, and a single parameter (the rotational temperature) was used to optimize the fit. The excellent fit to the data shown in Fig. 3 is typical for the entire spectrum (which probes both $\Omega = 0.5$ and 1.5 and rotational states up to $J = 25.5$) and provides an unambiguous fingerprint of the NO($v = 13$) molecules redistributed among their rotational states after collision with the surface.

We also obtained REMPI spectra of the scattered molecules at very early times after the beginning of the oxidation of the clean copper surface by the beam of ground-state NO. This experiment revealed that the survival of specific states of highly vibrationally excited NO is significantly reduced when the oxygen adlayer is removed from the surface. The dependence of the REMPI signal for molecules scattered into $v = 13$ (vibrationally elastic channel) upon exposure of the surface to ground-state NO could be fit to the

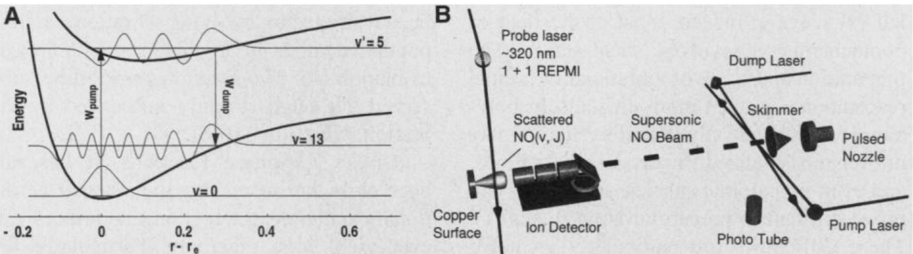

Fig. 1. (**A**) Schematic representation of the stimulated emission pumping method. Shown are two diatomic electronic states, as well as the dependence of their energies on the displacement of the atomic separation, *r*, from the equilibrium value, r_e. Molecules are excited out of ground-state levels through an allowed transition to an excited electronic state with a distorted structure. Laser-induced emission transfers population back to single highly vibrationally excited quantum states of the ground electronic state. Three realistic vibrational wave functions are shown. Energies accessible with this method can be large (>400 kJ/mol) and pumping can be efficient (~10^{-1} to 10^{-2}). (**B**) Experimental detail. Pump and dump lasers prepare highly vibrationally excited NO in the second differential pumping chamber downstream from a pulsed molecular beam of NO (seeded in He or H_2). A photomultiplier tube is used for fluorescence dip spectroscopy, which helps to control the optical excitation step. Pump laser–induced fluorescence is also monitored by a photomultiplier for signal normalization. The excited molecules travel through one more region of differential pumping and collide with a well-characterized copper surface or oxygen adlayer on copper. Scattered NO is state-selectively ionized using 1+1 resonance-enhanced multiphoton ionization. The ions are extracted back along the molecular beam direction and deflected to a microchannel plate detector. By scanning the frequency of the probe laser, we could measure the vibrational and rotational state distribution of the products. Translational energy distributions of the products are measured by recording the intensity of the REMPI signal as a function of the time delay between the excitation and probe lasers. Angular distributions were recorded by translating the probe laser across the direction of the incident molecular beam.

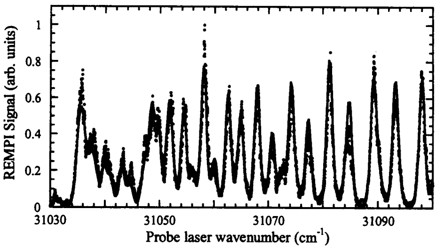

Fig. 2. REMPI spectrum of NO($v = 13$) scattered from an oxygen adlayer on Cu(111). The points are the data; the solid line is a least squares fit to the data. Only a portion of the spectrum is shown near the P_{12} and P_{22} band heads.

theoretical (first-order kinetics) expression $S(\sigma) = S(\infty) \times [1 - \exp(-K\sigma)] + S(0)$ (Fig. 3), where σ, represents the surface exposure to NO in monolayers (ML) (*22*), $S(\sigma)$ is the coverage-dependent REMPI signal, K is a rate constant, and S(0) is the REMPI signal obtained in the limit of zero exposure. The asymptotic magnitude of the REMPI signal is given by $S(\infty) + S(0)$. The survival probability as a function of surface exposure to NO is therefore $S(\sigma)/[S(0) + S(\infty)]$.

There are two possible explanations for the observation shown in Fig. 3. First, vibrationally inelastic channels could be significantly more probable on the clean copper surface relative to the oxidized surface. If this is the case, the "missing $v = 13$ signal" at low exposures should appear as enhanced signal for other vibrational states. That is, we expect in this case to observe a decrease in signal with exposure for lower energy vibrational states that are populated by the supposed enhanced vibrationally inelastic energy transfer. The second possible explanation for the diminished signal at low exposures is that the highly vibrationally excited NO reacts, thereby sticking to the clean copper surface, but cannot react as rapidly (if at all) on the oxidized surface. In this case we would expect to see a growth in all of the inelastic channels with exposure as the surface is transformed from its reactive form (copper) to its inactive form (oxidized copper).

We failed to find any inelastic channels that exhibited a dependence to surface NO exposure different from that shown in Fig. 3, despite our sensitive detection of many inelastic channels (*23*). Indeed, for a fixed surface temperature, all of the growth curves were quantitatively identical, which suggests that they reflect the same kinetic process: reaction of highly vibrationally excited NO on a clean copper surface. Presumably, oxidation of the copper surface by ground-state NO removes the sites where reaction of highly excited NO can take place. Thus, for oxidized surfaces, inelastic channels dominate.

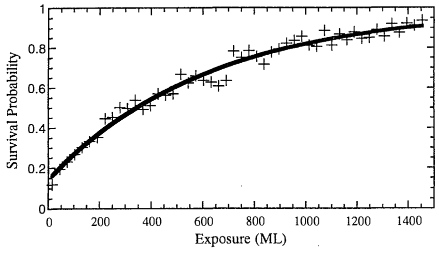

Fig. 3. Survival probability, $S(\sigma)/[S(0) + S(\infty)]$, of NO($v = 13$) as a function of surface exposure to the oxidizing action of ground-state NO. The increase in survival probability is explained by decreased reactivity of highly vibrationally excited NO on the O-covered copper surface.

On the basis of this interpretation, we can experimentally derive the reaction probability of highly vibrationally excited NO with a Cu(111) surface, $P_{\text{react}} = S(\infty)/[S(0) + S(\infty)]$. This analysis yields a value of 0.87 ± 0.05 for the data shown in Fig. 3 (*24*). That is, there is an 87% chance of reaction for NO($v = 13$) on Cu(111). A similar value was obtained for NO($v = 15$). Moreover, the reaction probability was found to be independent of the surface temperature and the translational energy of the molecular beam over the range studied (*25*).

To compare the rate of NO($v = 13, 15$) reaction on Cu(111) with that for NO($v = 0$), we measured the O AES signal versus exposure for ground-state NO. The oxygen coverage as a function of NO exposure exhibited first-order kinetics: $I(\sigma) = I(\infty) \times [1 - \exp(-k\sigma)]$. Here, $I(\sigma)$ is the intensity of the oxygen peak (at 510 V in AES) normalized to the intensity of the Cu peak (at 920 V). As before, σ stands for the NO exposure measured in ML. $I(\sigma)$ is directly proportional to the oxygen coverage at the surface. Fitting the kinetic expression to the measurements, we obtained a value of $k \sim 8 \times 10^{-4}$ ML^{-1} for the rate of oxidation of Cu(111) by ground-state NO. Taking $I(\infty) = 0.3$ ML as the saturation coverage of oxygen at Cu(111) (*16*), we could estimate the reaction probability at zero coverage for ground-state NO on Cu(111) $[k \times I(\infty)]$ to be 2×10^{-4}. This shows that vibrational excitation of NO enhances the probability of reaction by more than three orders of magnitude.

In principle, the observed vibrationally enhanced sticking of NO on Cu(111) could be nondissociative (trapping and desorption) or dissociative (forming O and N atoms bound to copper). If trapping and desorption were important, one might observe a reduced scattering signal at zero oxygen coverage because the desorbing molecules would be spread over a large range of scattering angles and speeds. Moreover, if the trapped molecules had a long lifetime on the surface, they might be emitted in vibrational states even lower than those probed in this work (up to $\Delta v = -5$). However, in light of the experimental evidence, the trapping and desorption scenario appears counterintuitive. In essence, trapping results from the rapid removal of energy from the gas-phase molecule during the surface collision. Thus, it is commonly observed that trapping is strongly inhibited by increased translational energy of the gas-phase molecule and to a more modest extent inhibited by increased surface temperature (*26*). Although there have been no studies of such an effect, it appears reasonable that the addition of vibrational energy to the gas-phase molecule would (like translation and rotation) also inhibit trapping.

In contrast, the sticking probability measured in these experiments is independent of both initial translation energy and surface temperature, and is enhanced by vibrational excitation by more than three orders of magnitude. This result indicates a direct chemical reaction where the well-defined motion of the reactant has not been overwhelmed by energy transfer to the surface. Vibrational excitation of NO enhancing the dissociation of the NO bond is also intuitively appealing. Indeed, the large enhancement by vibration and weak dependence on translation are consistent with a "late" transition state (*27*), where the transition state resembles more closely the adsorbed products of the reaction than it does the reactants. The results shown here lay the groundwork for detailed studies of the nature of the transition states of many surface reactions, coupling high-level experiment and theory.

References and Notes

1. C. E. Hamilton, J. L. Kinsey, R. W. Field, *Annu. Rev. Phys. Chem.* **37**, 493 (1986).
2. A. Sinha, J. D. Thoemke, F. Crim, *J. Chem. Phys.* **96**, 372 (1992); D. W. Arnold, M. Korolik, C. Wittig, H. Reisler, *Chem. Phys. Lett.* **282**, 313 (1998); C. A. Michaels, A. S. Mullin, J. Park, J. Z. Chou, G. W. Flynn, *J. Chem. Phys.* **108**, 2744 (1998); R. L. Miller *et al.*, *Science* **265**, 1831 (1994).
3. For example, see C. T. Rettner, H. E. Pfnür, H. Stein, D. J. Auerbach, *J. Vac. Sci. Technol.* **A6**, 899 (1988).
4. For example, see M. Gostein, H. Parhikhteh, G. O. Sitz, *Phys. Rev. Lett.* **75**, 342 (1995).
5. B. N. J. Persson and J. W. Gadzuk, *Surf. Sci.* **410**, L779 (1998).
6. B. N. J. Persson and Ph. Avouris, *ibid.* **390**, 45 (1997).
7. X. Yang and A. M. Wodtke, *J. Chem. Phys.* **92**, 116 (1990).
8. In our experiment, we have taken the $B^2\Pi_{1/2} \leftarrow X^2\Pi_{1/2}(5,0)$ transition for the pump step. For NO in a supersonic expansion (rotational temperature ~5 K), it was possible to transfer ~0.2% of the total population in the illuminated part of the molecular beam into the $v = 15$, $J = 2.5$ state.
9. M. Drabbels, A. M. Wodtke, M.-B. Yang, M. H. Alexander, *J. Phys. Chem.* **101**, 6463 (1997).
10. Single lines within the R_{11} branch of NO($B^2\Pi, v' = 5$) $\leftarrow$ NO($X^2\Pi, v'' = 0$) were excited in the pump step of the SEP. The laser light used for ω_{pump} was generated as follows. The output of an argon ion (Spectra Physics 171) pumped single-mode ring dye laser (Coherent CR-699) operated with Rhodamine 6G was pulse-amplified in a homemade three-stage amplifier chain, filled with a mixture of Rhodamine 610 and Rhodamine 640 dyes. The amplifier cuvettes were pumped by a frequency-doubled, Q-switched, injection-seeded Nd–yttrium-aluminum-garnet laser (Continuum Powerlite 7010-IS) with a pulse energy of 400 mJ at 532 nm and a pulse duration of ~5 ns. The amplified visible radiation was frequency-doubled in a KDP crystal to yield 15 mJ of ultraviolet light around 300 nm. After passing a λ/2 plate, the doubled and residual fundamental radiation were frequency-summed in a BBO crystal (length 1 cm) to yield light near 198 nm with a pulse energy of typically 0.5 to 1.0 mJ and a near-Fourier transform limited bandwidth of less than 150 MHz.
11. A XeCl pumped dye laser system (Lambda Physik EMG200MSC/FL3002) was used for the dump transitions.
12. The loss of side fluorescence to the photomultiplier tube due to enhanced stimulated emission along the dump laser propagation axis is referred to as a fluorescence dip. See, for example, (7).

13. Extreme care was taken to ensure that there were no impurities in the beam that might oxidize the surface.
14. M. H. Matloob and M. W. Roberts, *Phys. Scr.* **16**, 420 (1977).
15. The mechanism of oxidation is thought to be dissociative adsorption of NO. The removal of nitrogen adatoms may be explained in several ways: (i) reaction of adsorbed N atoms with NO in the molecular beam to form N_2O (which desorbs), (ii) the selective recombination of nitrogen adatoms to form desorbing N_2, or (iii) the reaction of two adsorbed NO molecules to form N_2O (which desorbs) + O, which is known to be important at low surface temperatures when the NO coverage is high.
16. The ratio of AES signals for Cu and O on this surface revealed a ratio of O adatom to surface Cu atom of ~1:3. This relied on a calibration of the AES response [F. H. P. M. Habraken, E. P. Kieffer, G. A. Bootsma, *Surf. Sci.* **83**, 45 (1979)].
17. M. Drabbels and A. M. Wodtke, *J. Chem. Phys.* **106**, 3024 (1997).
18. One photon excited the NO resonantly to the $A^2\Sigma^+$ state and a second photon ionized the molecules in the $A^2\Sigma^+$ state. For the experiments reported here, neither step of the REMPI process was saturated.
19. H. Hou *et al.*, *J. Chem. Phys.*, in press.
20. A significant background signal due to population of NO ($v = 13$) by the pump laser alone (known as Franck-Condon pumping background) has already been subtracted. This is done by analyzing the scattered REMPI signal with and without the dump laser. Because the dump transition induces a large fractional decrease in the population of the excited electronic level, $\delta n_{ex}/n_{ex}$ (~0.15), the net scattering signal is given as $S_{net} = S_3 - S_2[1 - (\delta n_{ex}/n_{ex})]$, where S_2 and S_3 are the two- and three-laser signals, respectively. $\delta n_{ex}/n_{ex}$ was measured from fluorescence dips. For analysis and display in Fig. 3, S_{net} was normalized to the square of the probe laser power.
21. After absolute wavelength calibration of the spectrum, the data shown here were fit using intermediate-case Hönl-London factors [R. N. Zare, *Angular Momentum* (Wiley-Interscience, New York, 1987), p. 314; note that the first P_2 branch in the table is actually the P_{21} branch]. Energy levels of the ground state are from C. Amiot, *J. Mol. Spectrosc.* **94**, 150 (1982). Energy levels for the *A* state derive from R. Engleman Jr., P. E. Rouse, H. M. Peek, V. D. Baiamonte, *Los Alamos Science Lab Report LA-4364* (1970); R. Engleman Jr. and P. E. Rouse, *J. Mol. Spectrosc.* **37**, 240 (1971). The rotational state populations were modeled by a Boltzmann distribution.
22. Here, one ML indicates 1.6×10^{15} molecules cm^{-2}.
23. The following channels were observed ($v = 15 \rightarrow 13$, $15 \rightarrow 10$, $13 \rightarrow 12$, $13 \rightarrow 10$, $13 \rightarrow 9$, $12 \rightarrow 9$).
24. Because of the difficulty of ensuring an absolutely oxygen-free surface and the high sensitivity of the REMPI signal to oxygen coverage, we consider this number to be a lower limit to the true value. The error bars represent one standard deviation.
25. Temperatures between 300 and 500 K were studied. Two molecular beams were compared with collision energies of 29 and 67 kJ/mol.
26. C. T. Rettner, D. J. Auerbach, J. C. Tully, A. W. Kleyn, *J. Phys. Chem.* **100**, 13021 (1996).
27. J. C. Polanyi, *Acc. Chem. Res.* **5**, 161 (1972); ——— and W. H. Wong, *J. Chem. Phys.* **51**, 1439 (1969).

28. Supported by the U.S. Air Force Office of Scientific Research (grant F49620-95-1-0234) and the U.S. Department of Energy Office of Basic Energy Sciences (grant DE-FG03-94ER14492/A000).

7 January 1999; accepted 5 May 1999

Adsorbed Layers and the Origin of Static Friction

Gang He, Martin H. Müser,* Mark O. Robbins†

Analytic results and experiments in ultrahigh vacuum indicate that the static friction between two clean crystalline surfaces should almost always vanish, yet macroscopic objects always exhibit static friction. A simple and general explanation for the prevalence of static friction is proposed. "Third bodies," such as small hydrocarbon molecules, adsorb on any surface exposed to air and can arrange to lock two contacting surfaces together. The resulting static friction is consistent with experimental behavior, including Amontons' laws.

Amontons' laws, which are 300 years old, state that the frictional force F needed to slide one body laterally over another is independent of their macroscopic area of contact and proportional to the normal load L that presses them together (*1, 2*). The constant of proportionality $\mu = F/L$, or coefficient of friction, depends on the materials and whether the bodies are at rest (μ_s) or in motion (μ_k).

Despite the success of Amontons' laws, there is no microscopic theory that explains their molecular origins and wide-ranging applicability. In fact, analytic theories indicate that static friction, the force F_s needed to initiate motion between two bodies at rest, should vanish between almost any pair of clean surfaces that deform elastically (*3–6*). These theories, and many simulation studies, only include atoms in the two bodies that move past each other. However, there is almost always some form of "third body" present between two surfaces. Indeed, Amontons measured static friction for greased surfaces (*1*), and any surface exposed to ambient air acquires an adsorbed layer of hydrocarbons and other small molecules that is a few angstroms thick. Larger particles may also be present in the form of dust or wear debris.

We report molecular dynamics simulations that show that third bodies naturally lead to a nonzero static friction. Moreover, the static friction produced by adsorbed layers of short molecules is consistent with Amontons' laws and does not vary substantially with parameters that are usually not controlled in experiments, such as the precise thickness and chemistry of adsorbed layers, the orientational alignment of the surfaces, and the direction of sliding relative to crystalline axes.

The actual area of molecular contact between two surfaces, A_{real}, is generally the small fraction of the apparent macroscopic area where peaks on opposing surfaces meet (*2, 7, 8*). Elastic deformation flattens the contact regions into micrometer diameter patches, orders of magnitude larger than individual molecules. The static friction corresponds to an average yield stress within these contacts of $\tau_s = F_s/A_{real}$.

Bowden and Tabor suggested a simple phenomenological form for τ_s that explains the successes of Amontons' laws and some of their failures (*2*). If the yield stress rises linearly with the local pressure $P = L/A_{real}$, then

$$\tau_s = \tau_0 + \alpha P \qquad (1)$$

One finds $F_s = \tau_0 A_{real} + \alpha L$ or

$$\mu_s = \alpha + \tau_0/P \qquad (2)$$

Thus, μ_s is independent of load and macroscopic area if P is constant or if P is much greater than τ_0. The former applies to simple models of ideally elastic (*9*) and plastic surfaces (*2*). Amontons' laws are known to fail when P varies substantially or τ_0 is large (strong adhesion), but Eqs. 1 and 2 remain valid (*10–13*).

The theoretical difficulty is that a nonzero τ_s requires that the surfaces lock together in a local free-energy minimum that prevents sliding (*3–6*). Every atom on two identical aligned crystals (Fig. 1A) can simultaneously lie at a local energy minimum and contribute coherently to τ_s. When the surfaces are rotated by almost any angle (Fig. 1, B and C) or have different lattice constants (Fig. 1D), the number of atoms resisting lateral motion is exactly equaled by the number assisting it. Such incommensurate surfaces have no static friction unless the interaction between them is so strong, compared to the interactions within the solids, that the surface atoms rearrange to create a local energy minimum (*3, 4, 14, 15*). Experimental studies of friction between clean crystalline surfaces are limited (*16*) but are consistent with this conclusion. Krim and co-workers measured no static friction between substrates and incommensurate adsorbed layers (*17*), and their data are consistent with simulations (*18*). Small crystalline atomic force microscope (AFM) tips show substantial static friction only at commensurate alignments (*19*). Finally, the friction between unaligned MoS_2 crystals is extremely low in ultrahigh vacuum but rises rapidly with exposure to air (*20*).

Third bodies such as airborne hydrocarbons

Department of Physics and Astronomy, Johns Hopkins University, Baltimore, MD 21218, USA.

*Present address: Institut für Physik, WA 331, Johannes Gutenberg-Universität, 55099 Mainz, Germany.

†To whom correspondence should be addressed: E-mail: mr@pha.jhu.edu